Separable Ernst-Shakin-Thaler expansions of local potentials

Gerhard Wilhelm Bund
Instituto de Física Teórica, CEP 01405 São Paulo, SP, Brasil
(Received 18 January 1985)

The boundary condition Ernst-Shakin-Thaler method, introduced previously to generate separable expansions of local potentials of finite range, is applied to the study of the triplet s-wave Malfliet-Tjon potential. The effect of varying the radius where the boundary condition is applied on the T matrix is analyzed. Further, we compare the convergence of the n-d scattering cross sections in the quartet state below the breakup threshold for expansions corresponding to two different boundaries.

I. INTRODUCTION

In a previous paper[1] we introduced separable Ernst-Shakin-Thaler (EST) expansions[2-4] of local potentials, using boundary conditions in order to generate the basis. This method, which we shall call BCEST, gives rigorous expansions for potentials of finite range, that is, potentials which vanish outside of a sphere of radius r_0.

More precisely it was established that, if one uses as a basis for the EST expansion the eigenstates of the Schrödinger equation subject to appropriate boundary conditions at a fixed radius ρ larger than the range r_0 of the potential, the separable EST series becomes exact; it gives us back the original potential. In Ref. 1 we studied also the rate of convergence of the separable T matrix for a square well potential for different values of the boundary radius ρ and found that the BCEST series converges rapidly towards the exact T matrix.

In the case of potentials which do not vanish outside of a given sphere, BCEST expansions will not converge towards the exact solution. Nevertheless, if the boundary is chosen such that in its exterior the potential becomes negligible, one expects that separable T matrices constructed according to the BCEST prescriptions should still yield good approximations to the exact T matrix. In order to investigate this question, we studied the BCEST expansions of the Malfliet-Tjon[5] triplet s-wave potential by comparing the corresponding T matrices with the exact ones, using ρ as an adjustable parameter. These comparisons are made for truncations of different ranks of the separable expansions, as we wish also to study the rate of convergence for different values of ρ. The boundary condition used was to fix the logarithmic derivative of the radial wave functions at ρ. In order that the exact T matrix at the bound-state pole be correctly reproduced by the separable T matrices, the value appropriate to the bound state was chosen.

Finally, we compared the performance of our two best separable expansions in neutron-deuteron scattering below the breakup threshold in the quartet state, assuming only the Malfliet-Tjon triplet s-wave nucleon-nucleon interaction to be present. In Sec. II we review the BCEST method and in Sec. III we present our numerical results for the two-nucleon and three-nucleon calculations; the method utilized in the calculation of the n-d scattering amplitude is presented in Refs. 10–13.

II. THE BCEST EXPANSION

Consider a complete basis of states Ψ_i, $i=1,2,\ldots,$ in the subspace of a fixed angular momentum. In this subspace we perform the following separable expansion[2] of the spherical potential V,

$$V=\sum_{i,j} V\,|\,\Psi_i\rangle M_{ij}\langle\Psi_j\,|\,V\,, \tag{1}$$

where the matrix M is given by

$$(M^{-1})_{ij}=\langle\Psi_i\,|\,V\,|\,\Psi_j\rangle\,. \tag{2}$$

Similarly, the off-shell T matrix may be written

$$T=\sum_{i,j} V\,|\,\Psi_i\rangle\tau_{ij}(E)\langle\Psi_j\,|\,V\,. \tag{3}$$

By making use of the Lippmann-Schwinger equation one gets[1,2] for the matrix τ the expression

$$(\tau^{-1})_{ij}=\langle\Psi_i\,|\,(V-VG_0^{(+)}V)\,|\,\Psi_j\rangle\,, \tag{4}$$

where

$$G_0^{(+)}(E)=(E-H_0+i\epsilon)^{-1}\,, \tag{5}$$

H_0 being the kinetic energy operator. The expansion of the R matrix is similarly obtained from Eqs. (3) and (4) through replacement of $G_0^{(+)}$ by $G_0^{(P)}$, the principal value Green's function in Eq. (4).

If $V(r)$ is a local spherical potential which vanishes for radii r larger than r_0, it may be seen that Eqs. (1)–(4) still hold[1] for a complete orthogonal basis of functions defined in the interior of a sphere of radius ρ larger than r_0. In the absence of tensor and spin orbit forces, these conditions are written

$$\sum_i \psi_i^*(r)\psi_i(r')=r^{-2}\delta(r-r'),\quad r<\rho,\quad r'<\rho\,, \tag{6}$$

$$\int_0^\rho r^2\psi_i(r)\psi_j(r)dr=\delta_{ij}\,, \tag{7}$$

where $\psi_i(r)$ denotes $\langle r\,|\,\Psi_i\rangle$. Further, in the particular case of EST expansions,[2] the states Ψ_i are required to be

TABLE I. ρ_α is the radius of the boundary and $V(\rho_\alpha)$ the corresponding value of the potential. $k_{E_i}^{(\alpha)2}$ $i=1,\ldots,5$ are the five lowest energies appropriate to the states of the BCEST basis; $E_1^{(\alpha)}=-2.23$ MeV.

α	ρ_α (fm)	$V(\rho_\alpha)$ (MeV)	$\lvert k_{E_1}^{(\alpha)}\rvert$ (fm^{-1})	$k_{E_2}^{(\alpha)}$ (fm^{-1})	$k_{E_3}^{(\alpha)}$ (fm^{-1})	$k_{E_4}^{(\alpha)}$ (fm^{-1})	$k_{E_5}^{(\alpha)}$ (fm^{-1})
a	3.48	-8.11	0.232	1.23	2.27	3.27	4.23
b	4.84	-0.71	0.232	0.83	1.57	2.29	2.98
c	8.30	-2×10^{-4}	0.232	0.43	0.86	1.27	1.68

eigenstates of the Schrödinger equation

$$(H_0+V-E_i)\,|\Psi_i\rangle=0\ . \tag{8}$$

A convenient way to obtain a complete orthogonal set of functions satisfying Eq. (8) in the interval $0<r<\rho$, is to impose linear boundary conditions at ρ,

$$\psi_i'(\rho)/\psi_i(\rho)=L,\quad i=1,2,\ldots\ . \tag{9}$$

Equations (8) and (9) generate a countable set of functions ψ_i. In order to be useful in the calculation of the n-d scattering amplitude, L is chosen equal to the logarithmic derivative of the radial wave function of the bound state. Thus the only adjustable parameter left is the radius ρ. As discussed in the Introduction, even if the potential does not strictly vanish outside the boundary, the expansions defined by Eqs. (3), (4), (8), and (9) may still represent a good approximation to the exact T matrix.

We next summarize the procedure followed in the calculation of the exact and separable T matrices. We found it more convenient to start with the R matrix, which is real. For this purpose we use the Kowalski-Noyes method[6,7] which consists in solving the integral equation

$$B(k,k',E)=V(k,k')+\int_0^\infty \Lambda(k,q,E)B(q,k',E)dq\ , \tag{10}$$

where

$$V(k,k')=\langle k\,|\,V\,|\,k'\rangle\ , \tag{11}$$

$|\,k\,\rangle$ being the free particle state corresponding to the energy k^2 ($\hbar^2/M_n=1$). The modified Lippmann-Schwinger kernel used in Eq. (10) for $E>0$,

$$\Lambda(k,q,E)=[V(k,q)-V(k,k_E)V_E^{-1}V(k_E,q)]\frac{q^2}{E-q^2}\ , \tag{12}$$

is nonsingular. Here $k_E^2=E$ and $V(k_E,k_E)$ is denoted by V_E. The off-shell R matrix is given directly[8] in terms of $B(k,k',E)$ and the T matrix is obtained from the R matrix by utilizing the Heitler relation.[9]

We consider now the separable R matrix. As the ex-

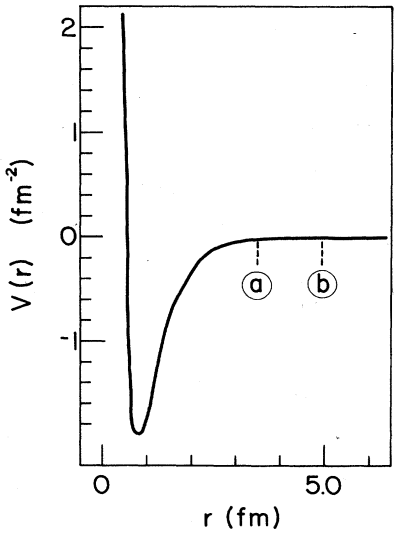

FIG. 1. The Malfliet-Tjon potential versus radius. The radii ρ_a and ρ_b where the logarithmic derivative of the radial wave function is fixed are indicated.

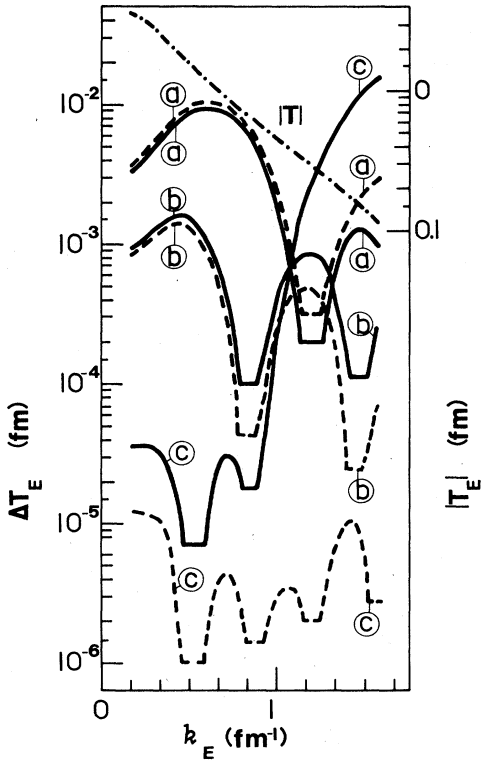

FIG. 2. $\Delta T_{E,\alpha}^{(N)}=|\,T_{E,\alpha}^{(N)}-T_E\,|$, the magnitude of the difference between the separable and the exact on-shell T matrix vs $k_E=E^{1/2}$ (1 fm^{-2}=41.5 MeV) for $N=3$ (full curves) and $N=5$ (dashed curves). The dot-dashed curve is the magnitude of the exact T matrix. The plateaus correspond to the zeros.

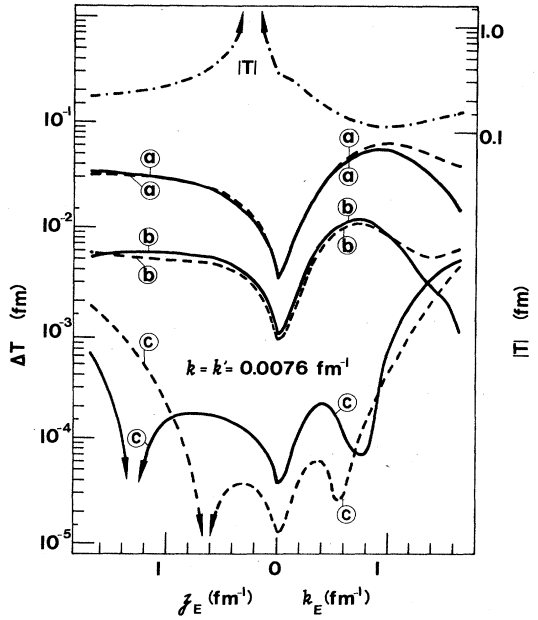

FIG. 3. The magnitude of the difference between the separable and the exact off-shell T matrix $|T_\alpha^{(N)}(k,k',E) - T(k,k',E)|$ vs $k_E = E^{1/2}$ $(E>0)$ and $\mathcal{I}_E = (-E)^{1/2}$ $(E<0)$ for $k = k' = 0.0076$ fm^{-1}, $N=3$ (full curves) and $N=5$ (dashed curves). The dot-dashed curve represents the magnitude of the exact off-shell T matrix $T(k,k',E)$. The arrows indicate zeros or infinites.

pressions (3) and (4) do not depend on the normalization of the states Ψ_i, we may define these states through the equation

$$|\Psi_i\rangle = \theta(E_i)\,|k_{E_i}\rangle + G_0^{(P)}(E_i)V\,|\Psi_i\rangle\ , \tag{13}$$

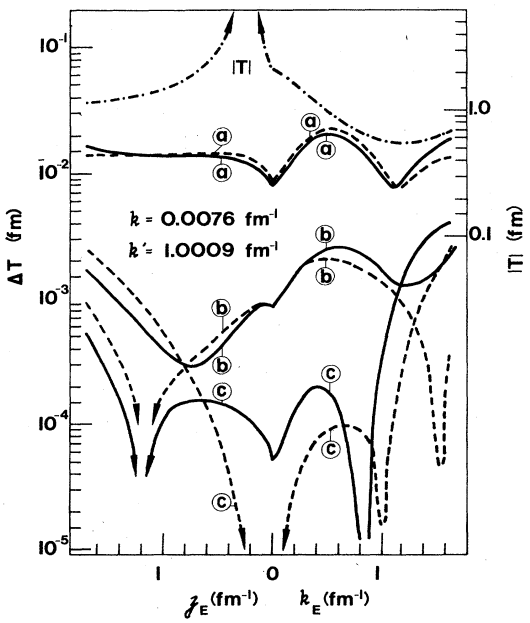

FIG. 4. As Fig. 3 for $k = 0.0076$ fm^{-1}, $k' = 1.0009$ fm^{-1}.

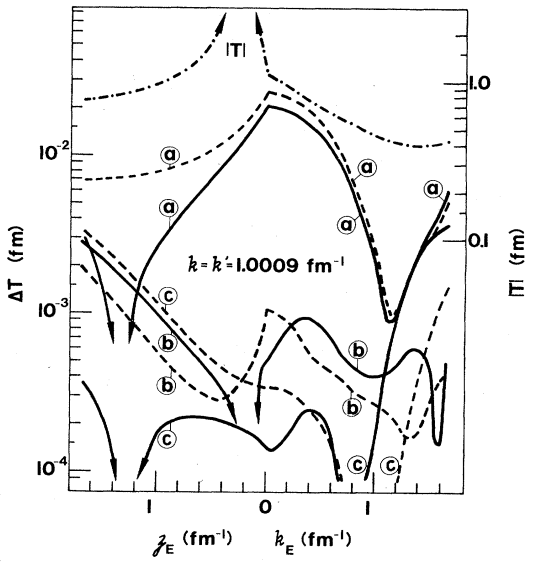

FIG. 5. As Fig. 3 for $k = 1.0009$ fm^{-1}, $k' = 1.0009$ fm^{-1}.

where $\theta(x)$ is the step function which vanishes if $x<0$ and equals 1 if $x>0$. In the momentum representation Eq. (13) becomes

$$\langle k\,|\,\Psi_i\rangle = \theta(E_i)\delta(k-k_{E_i})k^{-2} + (E_i - k^2)^{-1}R_i(k)\ , \tag{14}$$

where

$$R_i(k) = \langle k\,|\,V\,|\,\Psi_i\rangle\ , \tag{15}$$

which for positive energies, E_i is the exact half on-shell R matrix. The substitution of Eq. (14) into the first term on the right-hand side of Eq. (4) gives[8]

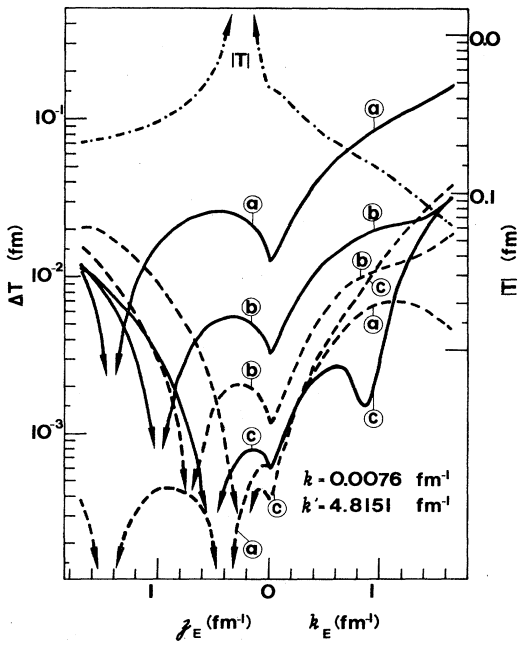

FIG. 6. As Fig. 3 for $k = 0.0076$ fm^{-1}, $k' = 4.8151$ fm^{-1}.

$$\langle \Psi_i \mid V \mid \Psi_j \rangle = \theta(E_i) R_j(k_{E_i}) + \int_0^\infty dk (E_i - k^2)^{-1} [k^2 R_i(k) R_j(k) - \theta(E_i) k_{E_i}^2 R_i(k_{E_i}) R_j(k_{E_i})], \quad E_j \geq E_i \ , \tag{16}$$

and for the second term one gets from Eq. (15) with $G_0^{(+)}$ replaced by $G_0^{(P)}$;

$$\langle \Psi_i \mid V G_0^{(P)} V \mid \Psi_j \rangle = \int_0^\infty dk (E - k^2)^{-1} [k^2 R_i(k) R_j(k) - \theta(E) k_E^2 R_i(k_E) R_j(k_E)] \ . \tag{17}$$

Thus we see that the separable off-shell R matrix may be written explicitly in terms of the exact half-shell and on-shell R matrices corresponding to the energy eigenvalues E_i.

III. NUMERICAL RESULTS

In this section we present the results obtained by using BCEST expansions for the Malfliet-Tjon potential.[5] We selected three cases which will be characterized by the additional index α, $\alpha = a,b,c$. In Table I we give the radii ρ_α where the logarithmic derivatives are fixed and the BCEST energy eigenvalues $E_i^{(\alpha)}$; $i = 1,2, \ldots,$ up to $i = 5$. The separable EST potentials of rank N generated by the N lowest eigenvalues $E_i^{(\alpha)}$ will be denoted by $V_\alpha^{(N)}$ and the corresponding T matrices by $T_\alpha^{(N)}$. These potentials correspond to truncate the summations in Eqs. (1) and (3) at the Nth term. As the first eigenvalues $E_1^{(\alpha)}$ are all equal to the energy of the bound state, for rank 1 our potentials become identical with the unitary pole approximation (UPA).[14]

As can be seen from Fig. 1 and from the values of $V(\rho_\alpha)$ in Table I; the potential $V(r)$ is already quite small for $r > \rho_b$ and becomes negligible for $r > \rho_c$. The value ρ_c was obtained by making the second eigenvalue $E_2^{(c)}$ equal to the energy where the scattering phase shift becomes equal to $\pi/2$. Thus it is expected that the potentials $V_c^{(N)}$ should, for large N, get very close to the exact potential. Consider

$$M_N^c = \max \mid V(k,k') - V_c^{(N)}(k,k') \mid \ , \tag{18}$$

the maximum deviation of the matrix elements of the potential as k and k' are varied. We obtained the values $M_5^c = 0.3$ fm and $M_{11}^c = 0.04$ fm. Considering that $\max \mid V(k,k') \mid = 1.7$ fm, one sees that $V_c^{(N)}$ gets close to V but that this convergence is rather slow. For the T matrix the convergence is much faster for energies E smaller or comparable to the largest energy eigenvalue $E_N^{(\alpha)}$.

In Fig. 2 we plot $\Delta T_{E,\alpha}^{(N)}$, the magnitude of the difference between the separable and the exact on-shell T matrices vs k_E. One verifies that $\Delta T_{E,\alpha}^{(N)}$ vanishes at the eigenvalues $E_i^{(\alpha)}$ (cf. Table I) as required by the EST condition, Eq. (8). We found that, for values of k_E up to 1 fm^{-1}, the T matrices $T_{E,a}^{(N)}$ give worse approximations to the exact T matrix than $T_{E,b}^{(N)}$ and $T_{E,c}^{(N)}$, and also that $T_{E,a}^{(N)}$ does not improve as N increases beyond $N = 3$.

In Figs. 3–8 we plot $\Delta T_\alpha^{(N)}(k,k',E)$, the magnitude of the difference between the separable and the exact off-shell T matrices for ranks 3 and 5 vs k_E for three values of the momenta k and k'. As can be verified from Figs. 3–5 we found that if the momenta k, k', and k_E are roughly less than 1 fm^{-1}, the best results belong to case c and the worst to case a. We obtained further for k and k' less than 1 fm^{-1}, irrespective of the values of E, that, again, there is practically no improvement of the T matrices $T_a^{(N)}$ for N larger than 3, as can be checked by comparing $T_a^{(3)}$ with $T_a^{(5)}$ in Figs. 3–5. We thus conclude that for momenta k and k' less than 1 fm^{-1} the maximum accuracy of the sequence $T_a^{(N)}$ has been attained essentially at rank 3.

We now consider momenta k or k' greater than 1 fm^{-1}, corresponding to Figs. 6–8. As can be seen from these figures, for $N \leq 3$, on the average, case c still gives the best results provided $\mid k_E \mid \lesssim 1$ fm^{-1}, but for $N \geq 5$, except at some narrow energy intervals, the best results belong to case a. Thus for the larger momenta the T-matrix sequences $T_a^{(N)}(k,k',E)$ converge faster. In particular, if both k and k' are large (Fig. 8), one finds that $T_a^{(3)}$

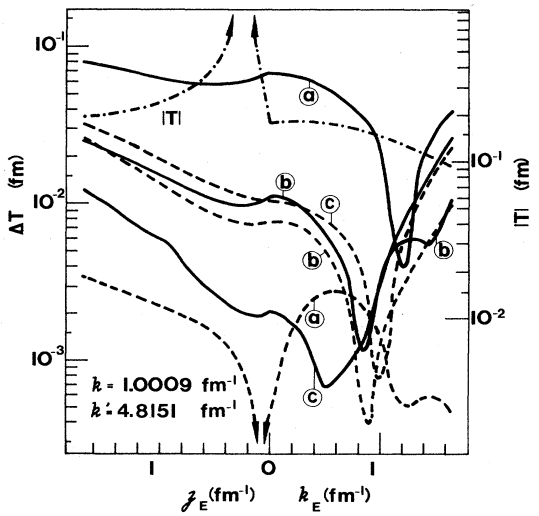

FIG. 7. As Fig. 3 for $k = 1.0009$ fm^{-1}, $k' = 4.8151$ fm^{-1}.

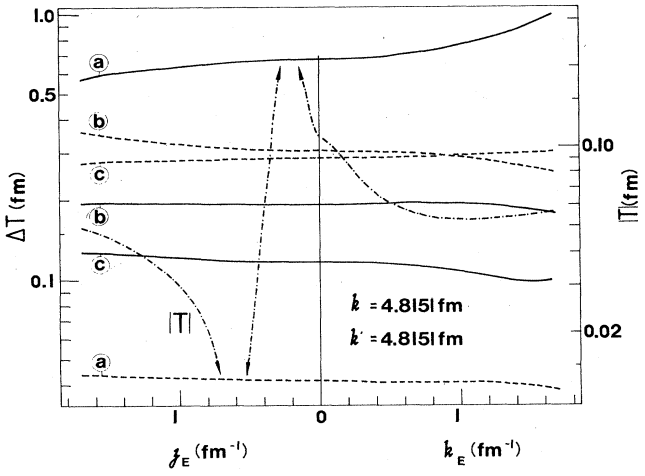

FIG. 8. As Fig. 3 for $k = 4.8151$ fm^{-1}, $k' = 4.48151$ fm^{-1}.

TABLE II. $a_b^{(N)}$ ($a_c^{(N)}$) are the n-d scattering lengths in the quartet state obtained by using the BCEST potentials $V_b^{(N)}$ ($V_c^{(N)}$) for the nucleon-nucleon interaction.

N	$a_b^{(N)}$ (fm)	$a_b^{(N)}-a_b^{(3)}$	$a_c^{(N)}$ (fm)	$a_c^{(N)}-a_c^{(3)}$
1	6.446 74	0.006 90	6.446 74	0.007 57
2	6.440 28	0.000 44	6.439 28	0.000 11
3	6.439 84		6.439 17	

gives the worst and $T_a^{(5)}$ the best results, the T matrix being now almost independent on E.

These results may be partly interpreted by considering that, with regard to a fixed momentum k, k', or k_E, the most relevant states of the basis are those for which the momenta k_{E_i} lie close to it. Thus the fact that the radius ρ_a is not large enough to generate a basis containing states with small momenta k_{E_i} (cf. Table I) explains why for the smaller momenta the T matrices $T_a^{(N)}$ give poor results. It also becomes clear why $T_a^{(5)}$ performs well for the larger values of k and k', as $k_{E_5}^{(a)}$ is sufficiently large to reach these momenta.

On the other hand, as ρ_c is the largest of the three radii, for almost all values of k, k', and E, we expect the T matrices $T_c^{(N)}$ to yield the best values, provided N is taken sufficiently large, a result that was borne out by calculations we made for $N>5$. As a check of our conclusions we truncated the local potential $V(r)$ at $r=\rho_a$. The error introduced in the on-shell T matrix by this truncation for small energies was indeed found to be of the same order of magnitude as the deviations $\Delta T_{E,a}^{(3)}$.

We consider finally the results we obtained in our test of n-d scattering in the quartet channel. For the nucleon-nucleon interaction we used the potentials $V_b^{(N)}$ and $V_c^{(N)}$ considering ranks 1, 2, and 3 only. The scattering lengths $a_\alpha^{(N)}$ are given in Table II; as can be seen the value corresponding to $N=1$ is very close to the exact result. The values of the deviations $a_\alpha^{(N)}-a_\alpha^{(3)}$ indicate a faster convergence in the case $\alpha=c$. In Fig. 9 we present the differences $|\sigma_\alpha^{(N)}-\sigma_\alpha^{(3)}|$, $\sigma_\alpha^{(N)}(\theta)$ being the differential scattering cross sections at 0.1 MeV below the breakup threshold. Again these results are consistent with a faster convergence in case c in agreement with our previous conclusions that up to the third rank the two-body T matrix corresponding to case c is on the average the best.

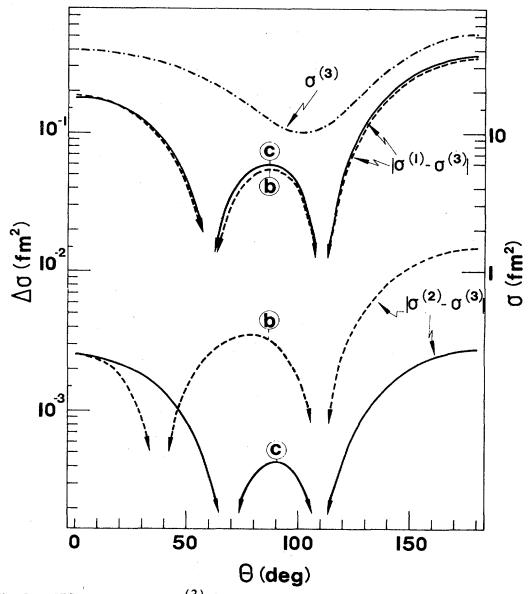

FIG. 9. We present $\sigma_c^{(3)}$ (dot-dashed curve) and the deviations $|\sigma_\alpha^{(N)}-\sigma_\alpha^{(3)}|$ vs the angle for $N=1,2$ in the cases $\alpha=b$ (dashed curves) and $\alpha=c$ (full curves), $\sigma_\alpha^{(N)}(\theta)$ being the n-d differential cross section at -0.1 MeV.

Our study indicates that BCEST expansions may be a useful tool for solving three-body problems although further research is required to settle the question of the best boundary. As a final remark we mention that our method can be applied also if from the start a separable representation of the local potential is used[3,4] as the role of the boundary condition is to supply the expansion energies.

This work was supported by Financiadora de Estudos e Projetos, Brasil.

[1]G. W. Bund and M. C. Tijero, Nuovo Cimento **57A**, 234 (1980).
[2]D. J. Ernst, C. M. Shakin, and R. M. Thaler, Phys. Rev. C **8**, 46 (1973).
[3]S. K. Adhikari, Phys. Rev. C **10**, 1623 (1974).
[4]S. C. Pieper, Phys. Rev. C **9**, 883 (1974).
[5]R. A. Malfliet and J. A. Tjon, Nucl. Phys. **A127**, 161 (1969).
[6]K. L. Kowalski and D. Feldman, J. Math. Phys. **4**, 507 (1963).
[7]H. P. Noyes, Phys. Rev. Lett. **15**, 538 (1965).
[8]G. W. Bund and H. A. Consoni, Rev. Bras. Fis. **6**, 297 (1976).
[9]K. M. Nutall and J. Watson, *Topics in Several Particle Dynamics* (Holden-Day, San Francisco, 1967), p. 19.
[10]C. Lovelace, Phys. Rev. **135**, B1225 (1964).
[11]E. O. Alt, P. Grassberger, and W. Sandhas, Nucl. Phys. **B2**, 167 (1967).
[12]T. Frederico, Tese de Mestrado, University of São Paulo, 1980 (unpublished).
[13]P. Doleschall, Nucl. Phys. **A201**, 264 (1973).
[14]E. Harms, Phys. Rev. C **1**, 1667 (1970).